

FULL PAPER

Open Access



# High-resolution regional gravity field recovery from Poisson wavelets using heterogeneous observational techniques

Yihao Wu<sup>1</sup>, Zhicai Luo<sup>1,2\*</sup>, Wu Chen<sup>3</sup> and Yongqi Chen<sup>3</sup>

## Abstract

We adopt Poisson wavelets for regional gravity field recovery using data acquired from various observational techniques; the method combines data of different spatial resolutions and coverage, and various spectral contents and noise levels. For managing the ill-conditioned system, the performances of the zero- and first-order Tikhonov regularization approaches are investigated. Moreover, a direct approach is proposed to properly combine Global Positioning System (GPS)/leveling data with the gravimetric quasi-geoid/geoid, where GPS/leveling data are treated as an additional observation group to form a new functional model. In this manner, the quasi-geoid/geoid that fits the local leveling system can be computed in one step, and no post-processing (e.g., corrector surface or least squares collocation) procedures are needed. As a case study, we model a new reference surface over Hong Kong. The results show solutions with first-order regularization are better than those obtained from zero-order regularization, which indicates the former may be more preferable for regional gravity field modeling. The numerical results also demonstrate the gravimetric quasi-geoid/geoid and GPS/leveling data can be combined properly using this direct approach, where no systematic errors exist between these two data sets. A comparison with 61 independent GPS/leveling points shows the accuracy of the new geoid, HKGEOD-2016, is around 1.1 cm. Further evaluation demonstrates the new geoid has improved significantly compared to the original model, HKGEOD-2000, and the standard deviation for the differences between the observed and computed geoidal heights at all GPS/leveling points is reduced from 2.4 to 0.6 cm. Finally, we conclude HKGEOD-2016 can be substituted for HKGEOD-2000 for engineering purposes and geophysical investigations in Hong Kong.

**Keywords:** Regional gravity field recovery, Poisson wavelets, Tikhonov regularization, Quasi-geoid/geoid, GPS/leveling data

## Background

High-resolution regional gravity field recovery is of considerable importance not only for surveying and mapping, but also for research fields, such as oceanography (understanding ocean circulation and currents), geophysics (investigating the structure of seismic activities and the lithosphere), and geodynamics (Kuroishi 2009; Panet et al. 2011; Shih et al. 2015).

Typically, middle- and short-wavelength gravity field signals down to a few kilometers are extracted from high-resolution ground-based measurements, e.g., terrestrial and shipborne gravity data, which are only available in geographically limited regions (Wang et al. 2012; Odera and Fukuda 2014; Lieb et al. 2016). In contrast, long-wavelength signals from tens of kilometers or larger are often recovered using global geopotential models (GGMs) derived from satellite observations. Over the last 10 years, launches of the Gravity Field and Climate Experiment (GRACE) (Tapley et al. 2004) and Gravity Field and Steady-State Ocean Circulation Explorer (GOCE) (Rummel et al. 2002) missions have greatly contributed to improving the spatial resolution and accuracy

\*Correspondence: zhcluo@sgg.whu.edu.cn

<sup>1</sup> MOE Key Laboratory of Fundamental Physical Quantities Measurement, School of Physics, Huazhong University of Science and Technology, Wuhan 430079, China

Full list of author information is available at the end of the article

of GGMs. Moreover, developing various observational techniques, e.g., GPS, airborne gravimetric measurements, and satellite altimetry missions, can further improve regional gravity fields (Hwang et al. 2006; Jiang and Wang 2016; Wu and Luo 2016). Combined, these data sets form a solid basis for modeling high-resolution and high-quality regional gravity fields. However, these data have heterogeneous spatial coverage and resolutions, various error characteristics, and different spectral contents, which make their use an open issue. Thus, the aim of this study is to adopt an approach that combines heterogeneous data and extracts different spectral contents from various observational techniques for regional gravity field recovery.

The Stokes/Molodensky integral makes it difficult to combine heterogeneous data, while the least squares collocation (LSC) is numerically inefficient in managing cases that involve a large number of point-wise data (Wittwer 2009). The new gravity field described in this study is parameterized using Poisson wavelets. Poisson wavelets are radially symmetric basis functions that have localizing properties in both the spatial and frequency domains, which have been used extensively in regional gravity field modeling and potential field analysis (Tenzer and Klees 2008; Hayn et al. 2012; Bentel et al. 2013).

We also investigate several aspects that affect the solution quality derived from Poisson wavelets. To begin with, as heterogeneous data have different spatial coverage and resolutions, the derived least squares system from Poisson wavelets is typically ill-conditioned, where regularization is mandatory for deriving reliable results (Wittwer 2009). One of the key points that affect the quality of regularization is the choice of regularization matrices (Chambodut et al. 2005). Unlike using diagonal regularization matrices in global gravity field modeling from spherical harmonics (Kusche and Klees 2002), the regularization matrices derived from various constraints in regional scale are no longer entirely diagonal. The choice of regularization matrices may affect the solution quality, which is investigated in this study.

Moreover, mainly due to commission errors in the GGMs and uncorrected systematic errors in the data, the computed gravimetric quasi-geoid/geoid usually deviates from local values observed from GPS/leveling data by a centimeter level or larger (Wu et al. 2016). Generally speaking, corrector surface (Featherstone 2000; Fotopoulos 2005; Nahavandchi and Soltanpour 2006) or more complicated algorithms, e.g., least squares collocation (Tscherning 1978) and boundary-value methodology (Klees and Prutkin 2008; Prutkin and Klees 2008), can be applied to reduce systematic errors and properly combine GPS/leveling data and gravimetric solutions. However,

given the difficulty in choosing a proper corrector surface, as well as the associated algorithmic complexity for the least-squares collocation and boundary-value approach, we propose a direct methodology for removing the inconsistency between these two data sets. The GPS/leveling data are treated as an independent observation group and added to the functional model for the gravity field computation. Using this method, the quasi-geoid/geoid that fits the local leveling system is computed in one step, no systematic errors exist between the data, and post-processing procedures, e.g., corrector surface or LSC approaches, for calibrating systematic errors are not required.

The rest of the paper is organized as follows: the main principle of regional gravity modeling from Poisson wavelets is first introduced, and heterogeneous gravity-related observations are linked to the functional model parameterized by Poisson wavelets. The weights for different observation groups are determined through the variance component estimation (VCE) approach, and unknown coefficients are estimated through the least squares adjustment. Further, the Tikhonov regularization method is introduced to deal with the ill-conditioned system, where a rapid synthesis method for computing zero- and first-order regularization matrices is provided. In the following section, Hong Kong is selected as the study area and heterogeneous data are introduced. The numerical results are also shown in this part, where the new height reference surface, HKGEOID-2016, is determined. In addition, HKGEOID-2016 is compared with existing models, e.g., HKGEOID-2000 (Luo et al. 2005) and recently published GGMs, such as EIGEN-6C4 (European Improved Gravity Model of the Earth by New Techniques 6C4) and EIGEN-6C3STAT (Förste et al. 2012, 2014), for cross-validation. The last section contains the main summary and conclusions.

## Methods

### Functional model and parameters estimation

Following Holschneider and Iglesias-Nowak (2004), we denote  $\Omega_R$  as the sphere of radius  $R$ ,  $\Omega_R = \{(u_1, u_2, u_3): u_1^2 + u_2^2 + u_3^2 = R^2\}$ , and we also denote  $\text{Int}\Omega_R$  as the interior and  $\text{Ext}\Omega_R$  as the exterior:

$$\text{Int}(\text{Ext})\ \Omega_R = \left\{ (u_1, u_2, u_3): u_1^2 + u_2^2 + u_3^2 < (>)R^2 \right\} \quad (1)$$

Consider two points  $y, z, |y| < R < |z|$ , and then the exterior Poisson wavelet of degree  $d$  in position  $y$  evaluated at  $z$  is defined by (Holschneider and Iglesias-Nowak 2004)

$$W_y^{\text{ext},d}(z) = \frac{R}{|z|} \sum_{l=0}^{\infty} l^d \left( \frac{|y|}{|z|} \right)^l (2l+1) P_l(z^T \hat{y}) \quad (2)$$

where  $\mathbf{z} = (z_1, z_2, z_3)^T$ ,  $\mathbf{y} = (y_1, y_2, y_3)^T$ , and  $\hat{\mathbf{z}} = \frac{\mathbf{z}}{|\mathbf{z}|}$  and  $\hat{\mathbf{y}} = \frac{\mathbf{y}}{|\mathbf{y}|}$  are the unit vectors of  $\mathbf{z}$  and  $\mathbf{y}$ , respectively.

$P_l(\hat{\mathbf{z}}^T \hat{\mathbf{y}})$  is the Legendre function.

In the framework of remove-compute-restore (RCR) methodology, only the residual disturbing potential is parameterized by Poisson wavelets, while the long- and short-wavelength parts of the gravity field are recovered using the global geopotential model (GGM) and residual terrain model (RTM), respectively (Omang and Forsberg 2000). Based on the Runge–Krarup theory, the residual disturbing potential,  $T_{\text{res}}$ , is estimated using a linear combination of Poisson wavelets (Klees et al. 2008):

$$T_{\text{res}}(\mathbf{z}) = \sum_{i=1}^K \beta_i W_{\mathbf{y}_i}^{\text{ext},d}(\mathbf{z}) \quad (3)$$

where  $\mathbf{z}$  and  $\mathbf{y}$  are interpreted as the 3-D coordinates of the observations and position of a Poisson wavelet, respectively.  $K$  is the number of Poisson wavelets,  $\beta_i$  is an unknown coefficient, which should be estimated from the data. Moreover,  $\Omega_R$  is chosen as a sphere that is entirely located within the Earth, e.g., a Bjerhammar sphere. We note that the depth of the Poisson wavelet under the Bjerhammar sphere, computed as  $d = R - |\mathbf{y}|$ , is the key point to determining its property in the frequency domain (Wittwer 2009).

After the linearization and spherical approximation, the residual gravity anomalies,  $\Delta g_{\text{res}}$ , can be linked to Poisson wavelets through (Klees et al. 2008)

$$\Delta g_{\text{res}}(\mathbf{z}) = \sum_{i=1}^K \beta_i \left( -\frac{\partial}{\partial |\mathbf{z}|} W_{\mathbf{y}_i}^{\text{ext},d}(\mathbf{z}) - \frac{2}{|\mathbf{z}|} W_{\mathbf{y}_i}^{\text{ext},d}(\mathbf{z}) \right) \quad (4)$$

The computed model, together with the RTM reduction, derives the quasi-geoid instead of geoid, and the residual height anomaly,  $\varsigma_{\text{res}}$ , is derived from Poisson wavelets using the Bruns formula (Heiskanen and Moritz 1967):

$$\varsigma_{\text{res}}(\mathbf{z}) = \sum_{i=1}^K \beta_i \frac{W_{\mathbf{y}_i}^{\text{ext},d}(\mathbf{z})}{\gamma(\mathbf{z})} \quad (5)$$

where  $\gamma$  is the normal gravity value.

In order to properly combine the gravimetric quasi-geoid/geoid and GPS/leveling data, parts of the GPS/leveling data,  $\varsigma_{\text{res}}^p$ , are treated as observations, which are added in the functional model for the regional gravity field computation:

$$\varsigma_{\text{res}}^p(\mathbf{z}) = \sum_{i=1}^K \beta_i \frac{W_{\mathbf{y}_i}^{\text{ext},d}(\mathbf{z})}{\gamma(\mathbf{z})} + \eta^T \chi \quad (6)$$

where  $\eta$  is the 7-parameter model, which is used to absorb systematic errors between these two data sets,

and  $\chi$  is a vector of unknown parameters. More specifically,  $\eta$  and  $\chi$  are expressed as (Eshagh and Zoghi 2016)

$$\eta = \begin{pmatrix} \cos\varphi \cos\lambda \\ \cos\varphi \sin\lambda \\ \sin\varphi \\ \cos\varphi \sin\varphi \cos\lambda / (1 - e^2 \sin^2\varphi)^{1/2} \\ \cos\varphi \sin\varphi \sin\lambda / (1 - e^2 \sin^2\varphi)^{1/2} \\ \sin^2\varphi / (1 - e^2 \sin^2\varphi)^{1/2} \\ 1 \end{pmatrix}; \quad \chi = \begin{pmatrix} \chi_1 \\ \chi_2 \\ \chi_3 \\ \chi_4 \\ \chi_5 \\ \chi_6 \\ \chi_7 \end{pmatrix} \quad (7)$$

where  $\varphi$  and  $\lambda$  are the latitude and longitude of the GPS/leveling data,  $e$  is the second eccentricity of the reference ellipsoid.

Typically, observations  $\mathbf{l}_p$  in group  $p$  are linked to the residual disturbing potential  $T_{\text{res}}(\mathbf{z})$  through

$$\mathbf{l}_p + \Delta_p + b_p = \mathbf{L}_p T_{\text{res}}(\mathbf{z}) = \sum_{i=1}^K \beta_i \mathbf{L}_p \Psi_i(\mathbf{z}, \mathbf{y}_i), \quad p = 1, 2, \dots, J \quad (8)$$

where  $\Delta_p$  are observation errors,  $b_p$  is an unknown bias parameter,  $\mathbf{L}_p$  is the specific function linking observations to the residual disturbing potential,  $J$  is the number of observation groups.

Assuming that the observation noise is white Gaussian with zero mean, Eq. (8) is rewritten as

$$\mathbf{l}_p - \mathbf{e}_p = \mathbf{A}_p \mathbf{x}, \quad E\{\mathbf{e}_p\} = 0, \quad D\{\mathbf{e}_p\} = \mathbf{C}_p = \sigma_p^2 \mathbf{Q}_p \quad (9)$$

where  $\mathbf{x}$  is the  $K' \times 1$  vector of unknown coefficients, which consists of unknown parameters of Poisson wavelets and bias parameters. For example,  $\mathbf{x} = [\beta_1, \beta_2, \dots, \beta_K, b_1, b_2, \dots, b_J]'$  and  $K' = K + J$ ,  $\mathbf{A}_p$  is the  $m_p \times K'$  design matrix of group  $p$ ,  $\mathbf{l}_p$  is the  $m_p \times 1$  corresponding observation vector,  $\mathbf{e}_p$  is the  $m_p \times 1$  vector of corresponding stochastic errors, and  $m_p$  is the number of observations in group  $p$ .  $E\{\cdot\}$  and  $D\{\cdot\}$  are the expectation and dispersion operators, respectively.  $\mathbf{C}_p$  is the error variance–covariance matrix of group  $p$ , and  $\sigma_p^2$  and  $\mathbf{Q}_p$  are the variance factor and cofactor matrix, respectively.

The observations in different groups are assumed to be uncorrelated, and the error variance–covariance matrix of all observation groups is expressed as

$$\mathbf{C} = \begin{pmatrix} \mathbf{C}_1 & 0 & 0 & \cdots & 0 \\ 0 & \mathbf{C}_2 & 0 & \cdots & 0 \\ \vdots & \vdots & \vdots & \ddots & \vdots \\ 0 & 0 & 0 & \cdots & \mathbf{C}_J \end{pmatrix} \quad (10)$$

Point-wise data can be directly linked to Poisson wavelets through the functional model described above. However, as these data are not homogeneously distributed and data gaps may exist in locally, the associated least squares system is typically ill-conditioned, and regularization is mandatory (Wittwer 2009). Usually, the Tikhonov regularization method is applied for tackling the ill-conditioned issues, because it does not need a priori information (Xu 1992). For a given  $\alpha$  (regularization parameter) and  $\kappa$  (regularization matrix), the least-squares solution of Eq. (9) is (Klees et al. 2008)

$$\hat{\mathbf{x}} = \left( \sum_{p=1}^J \mathbf{A}_p^T \mathbf{C}_p^{-1} \mathbf{A}_p + \alpha \kappa \right)^{-1} \left( \sum_{p=1}^J \mathbf{A}_p^T \mathbf{C}_p^{-1} \mathbf{l}_p \right) \quad (11)$$

The widely used L-curve approach, which is the log-log scale plot of the residual norm versus solution norm, is used to estimate the regularization parameter in this study. For discrete ill-conditioned problems, this plot displays an ‘L-shape’ with a corner point, where a certain balance between the regularized solution and fit to the data is achieved (Hansen et al. 2007). Moreover, the variance component estimation (VCE) approach can be applied to determine the optimal variance factors of different observation groups (Koch and Kusche 2002; Kusche 2003):

$$\hat{\sigma}_p^2 = \frac{\mathbf{v}_p^T \mathbf{Q}_p^{-1} \mathbf{v}_p}{r_p} \quad (12)$$

where  $\mathbf{v}_p = \mathbf{A}_p \hat{\mathbf{x}} - \mathbf{l}_p$  is the vector of residuals for group  $p$  and  $r_p$  is the corresponding redundancy number. The estimation of the variance factor is iteratively computed until convergence is achieved.

The final quasi-geoid,  $\varsigma$ , is computed by combining the residual part with the long- and short-wavelength components derived from the GGM ( $\varsigma_{\text{GGM}}$ ) and RTM ( $\varsigma_{\text{RTM}}$ ), respectively (Omang and Forsberg 2000):

$$\varsigma = \varsigma_{\text{GGM}} + \varsigma_{\text{RTM}} + \varsigma_{\text{res}} \quad (13)$$

However, the geoid ( $N$ ) instead of a quasi-geoid is needed in some cases, where their relationship is described by

$$N - \varsigma = \frac{\bar{g} - \bar{\gamma}}{\bar{\gamma}} h = \frac{\Delta g_B}{\bar{\gamma}} h \quad (14)$$

where  $\bar{g}$  and  $\bar{\gamma}$  are the mean value of gravity and normal gravity, respectively,  $\Delta g_B$  is the Bouguer anomaly, and  $h$  is topographical height.

#### Choice of regularization matrix

The regularization matrix is the key element controlling the quality of the regularized solutions, which describes

the signal energy decreasing from large to small scale (Chambodut et al. 2005). For selecting the optimal regularization matrix, the zero- and first-order regularization matrices are investigated.

#### Zero-order Tikhonov regularization

With the addition theorem of spherical harmonics, the Poisson wavelets are rewritten as (Wittwer 2009)

$$W_{\mathbf{y}}^{\text{ext},d}(\mathbf{z}) = \sum_{l=0}^{\infty} \sum_{m=-l}^l \psi_l \bar{Y}_{lm}(\hat{\mathbf{z}}) \bar{Y}_{lm}(\hat{\mathbf{y}}), \quad \psi_l = l^d \left( \frac{|R|}{|\mathbf{z}|} \right)^{l+1} \quad (15)$$

where  $\bar{Y}_{lm}$  are the fully normalized spherical harmonics,  $l$  and  $m$  are their degree and order, respectively.

If we assume Poisson wavelets are the target functions on the sphere, i.e.,  $s = W_{\mathbf{y}}^{\text{ext},d}(\mathbf{z})$ , then the entries of the zero-order regularization matrix  $\kappa_{P,Q}^0$  are expressed as the inner product of different Poisson wavelets (Heiskanen and Moritz 1967):

$$\kappa_{P,Q}^0 = \langle s_P, s_Q \rangle = \frac{1}{4\pi R^2} \int_{\Omega_R} W_{\mathbf{y}_P}^{\text{ext},d}(\mathbf{z}) W_{\mathbf{y}_Q}^{\text{ext},d}(\mathbf{z}) d\Omega_R \quad (16)$$

Equation (16) is also rapidly synthesized by Holschneider and Iglewska-Nowak (2004)

$$\left\langle W_{\mathbf{y}_P}^{\text{ext},d}, W_{\mathbf{y}_Q}^{\text{ext},d} \right\rangle = \frac{R}{|\mathbf{y}_P|} W_{\mathbf{y}_Q}^{\text{ext},2d}(\mathbf{y}_P^*) = \frac{R}{|\mathbf{y}_Q|} W_{\mathbf{y}_P}^{\text{ext},2d}(\mathbf{y}_Q^*) \quad (17)$$

where  $\mathbf{y}_P^* = \frac{R^2}{|\mathbf{y}_P|^2} \mathbf{y}_P$  and  $\mathbf{y}_Q^* = \frac{R^2}{|\mathbf{y}_Q|^2} \mathbf{y}_Q$ .

#### First-order Tikhonov regularization

The zero-order Tikhonov regularization derived above is suitable for functions restricted to a sphere  $\sigma_U$  belonging to  $L_2(\sigma_U)$ . However, this function space is quite large and includes many unsMOOTH functions. To introduce a scalar product suitable for smoother functions, a target function is selected as the first-order derivative of the Poisson wavelets, and the inner products of the target functions are used to derive the entries of the first-order regularization matrix.

Assuming the target function is a first-order radial derivative of the Poisson wavelets, the entries of the radially constrained regularization matrix  $\kappa_{P,Q}^r$  are (Heiskanen and Moritz 1967)

$$\kappa_{P,Q}^r = \frac{1}{4\pi R^2} \int_{\Omega_R} \frac{\partial W_{\mathbf{y}_P}^{\text{ext},d}(\mathbf{z})}{\partial |\mathbf{z}|} \frac{\partial W_{\mathbf{y}_Q}^{\text{ext},d}(\mathbf{z})}{\partial |\mathbf{z}|} d\Omega_R \quad (18)$$

As  $\frac{\partial}{\partial |\mathbf{z}|} \psi_l = -\frac{l+1}{|\mathbf{z}|} \psi_l$ , in Eqs. (15), (18) is rewritten as

$$\kappa_{P,Q}^r = \sum_{l=0}^{\infty} \psi_l^2 \left( \frac{l+1}{|\mathbf{z}|} \right)^2 (2l+1) P_l(\hat{\mathbf{y}}_P^T \hat{\mathbf{y}}_Q) \quad (19)$$

According to Holschneider and Iglewska-Nowak (2004),  $\kappa_{P,Q}^r$  is rapidly computed as

$$\kappa_{P,Q}^r = \frac{R}{|z|^2 |y_P|} \left( W_{y_Q}^{\text{ext},2d+2}(y_P^*) + 2W_{y_Q}^{\text{ext},2d+1}(y_P^*) + W_{y_Q}^{\text{ext},2d}(y_P^*) \right) \quad (20)$$

Similarly, the entries of the horizontal constrained regularization matrix  $R_{P,Q}^h$  read

$$\kappa_{P,Q}^h = \frac{R}{|z|^2 |y_P|} \left( W_{y_Q}^{\text{ext},2d+2}(y_P^*) + W_{y_Q}^{\text{ext},2d+1}(y_P^*) \right) \quad (21)$$

## Results and discussion

### Study area and data

The study area is bounded by  $113.83^\circ$  to  $114.5^\circ$  in longitude and from  $22.15^\circ$  to  $22.58^\circ$  in latitude, as shown in the region enclosed in a black rectangle in Fig. 1, which covers the entire Hong Kong mainland, parts of Shenzhen, as well as the South China Sea. Figure 1 also shows the distribution of heterogeneous gravity data; the red dots represent terrestrial data, including measurements both in Hong Kong and parts of Shenzhen. The green dots indicate locations of shipborne data coverage, which are sparsely distributed. As a result, we also incorporate satellite altimetry-derived gravity data to fill these data gaps, indicated with yellow dots, obtained from DTU13 (DTU = Technical University of Denmark) that uses multi-satellite altimetry data (e.g., TOPEX/Poseidon, Jason-1, Jason-2, ERS-2) over 20 years. DTU13 has a spatial resolution of  $1' \times 1'$ , and the altimetry gravity data precision is approximately several mGal globally (Andersen et al. 2013). We note that even the terrestrial data are not homogeneously distributed and data gaps exist, especially for mainland Hong Kong. This makes the study area a good location to test the feasibility of our adopted approach for managing data gaps. Because the currently used leveling system, Hong Kong Principal Datum (HKPD) over Hong Kong, is an orthometric

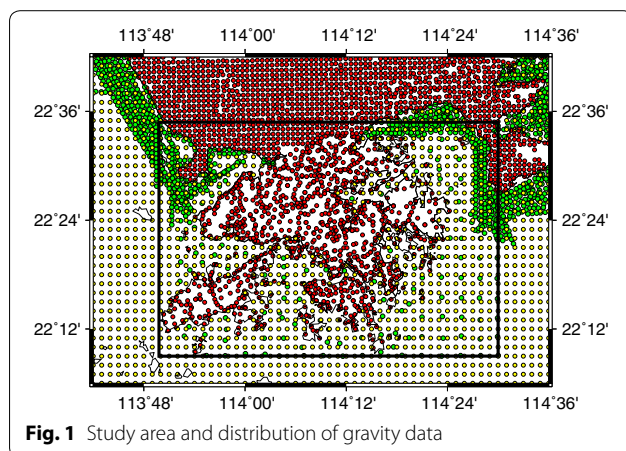
height system (Chen and Luo 2004), the modeled quasi-geoid from Eq. (13) is converted to a geoid for further validation and comparison.

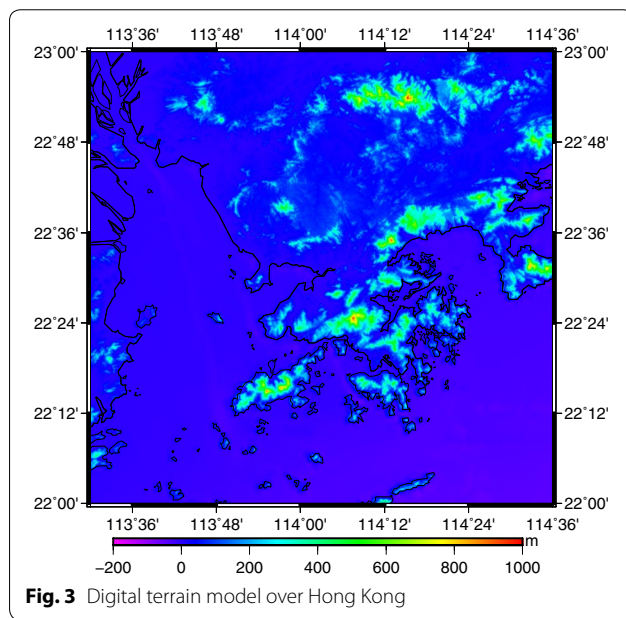
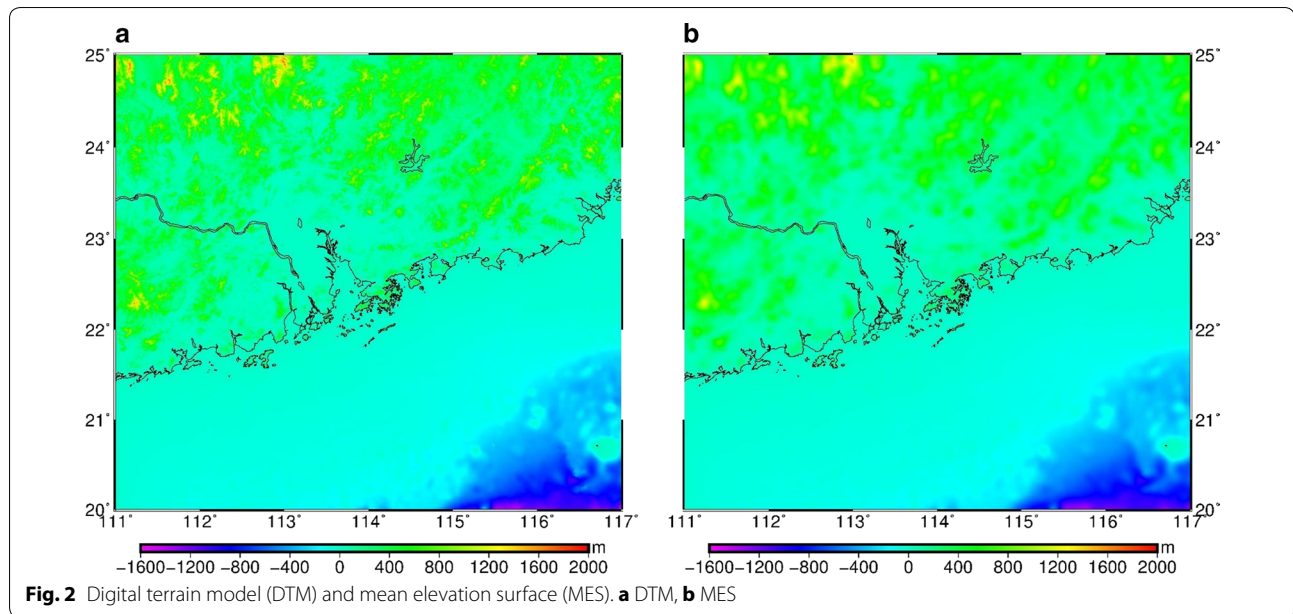
### Global geopotential model and digital terrain model

Earth Gravity Model 2008 (EGM2008) with a full degree and order (d/o) of 2190 (Pavlis et al. 2008, 2012) is chosen to recover long-wavelength signals of the regional gravity field. EGM2008 was developed by combining satellite gravity observations, ground-based gravity measurements and radar altimetry data; the accuracy of EGM2008 is 0.239 m when compared to globally distributed GPS/leveling data, which is one of the most accurate GGMs published in the recent years <http://icgem.gfz-potsdam.de/ICGEM/evaluation/evaluation.html>. A high-resolution and high-quality DTM (digital terrain model) is needed for applying RTM corrections to smooth the regional gravity field at short scales (Forsberg and Tscherning 1981). Two data sources, SRTM (Shuttle Radar Topography Mission) and GEBCO (General Bathymetric Chart of the Oceans), are combined to generate a DTM with a spatial resolution of three arc-seconds over land and sea. In order to reduce edge effects, a larger RTM computational area than study region is need; the derived DTM is shown in Fig. 2a. The mean elevation surface (MES) used in the RTM is computed from a high-order spherical harmonic expansion of Earth's topography, the DTM2006.0 topography model (Pavlis et al. 2007, 2008). The truncated degree of DTM2006.0 is consistent with the GGM used in this study, EGM2008 with a full d/o of 2190. The derived mean elevation surface is shown as Fig. 2b. Considering the curvature of Earth, tesseroids instead of prisms are chosen as the integral elements (Heck and Seitz 2007). The density parameter is selected as  $\rho_{\text{land}} = 2.67 \text{ g/cm}^3$  and  $\rho_{\text{sea}} = 1.64 \text{ g/cm}^3$  given the difference between the mean crustal density and seawater (Forsberg 1984). We also show detailed topographical information over Hong Kong (Fig. 3).

### GPS/leveling data

There are 168 high-quality GPS stations in Hong Kong, the ellipsoidal heights are referenced to the WGS84 ellipsoid (ITRF 96 @ 1998:121), and their heights were determined with precise geometric leveling and trigonometric leveling. The entire GPS/leveling dataset is divided into three groups (Fig. 4). The leveling heights of GPS/leveling data in the first group were derived from precise leveling measurement, while the heights of the next two groups were surveyed from precise leveling and trigonometric height measurements. Based on recent leveling network adjustments, the accuracy of the overall GPS/leveling data is approximately 1 cm. The first two groups, i.e., group I (58 points) and II (49 points), are used as





observations, aimed at reducing inconsistency between the gravimetric solution and GPS/leveling data. The third group (61 points), group III, is applied to evaluating the quality of the computed model.

#### Gravity data

The original gravity database in Hong Kong has 507 terrestrial and 133 shipborne point-wise gravity observations, the spacing on land is 2 and 2–4 km at sea. They were collected using a Lacoste and Romberg model 'G' land gravity meter and model 'H/U' seabed gravity meter

from Electronic and Geophysical Services Ltd (Luo et al. 2005). The local gravity base is connected to International Gravity Standardization Net 1971 (IGSN 71) with an accuracy of 0.03 mGal (Evans 1990). Moreover, recent gravity measurements also provide 623 discrete terrestrial gravity observations. The heights of gravity data in Hong Kong are referenced to the Hong Kong Principal Datum. In addition, gravity measurements in the neighboring Shenzhen region are also available, 1312 points on land and 876 points at sea, with 1 km spatial resolution. They were measured with a Lacoste & Romberg model 'G' and 'D' land gravimeter and model 'S' sea gravimeter in 2001, and the accuracy of observed data is better than 0.1 mGal. The heights of gravity measurements over Shenzhen are referenced to the National Vertical Datum 1956 (Chen and Luo 2004). Further, due to poor coverage of the marine gravity observations, DTU13-derived altimetry gravity anomalies are also introduced. The DTU13 model uses the EGM2008-derived geoid as the vertical datum (Andersen et al. 2013). To unify these heterogeneous gravity data from various sources, transforming parameters are used for height datum unification, and the heights of gravity data from Shenzhen and the DTU13 model are unified to the local heights based on the Hong Kong Principal Datum. To quantify the DTU13 model quality in the target region, DTU13-derived gravity anomalies are compared with marine gravity data (Fig. 5). The comparison indicates large differences in the coastal areas, where the quality of the altimetry data is suspect (Hwang et al. 2006). The statistics in Table 1 show the accuracy of the DTU13 model for the seas around Hong Kong is approximately 4.3 mGal.

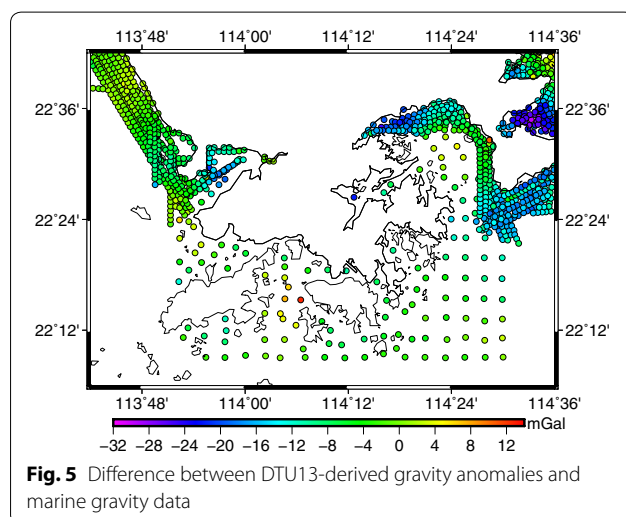
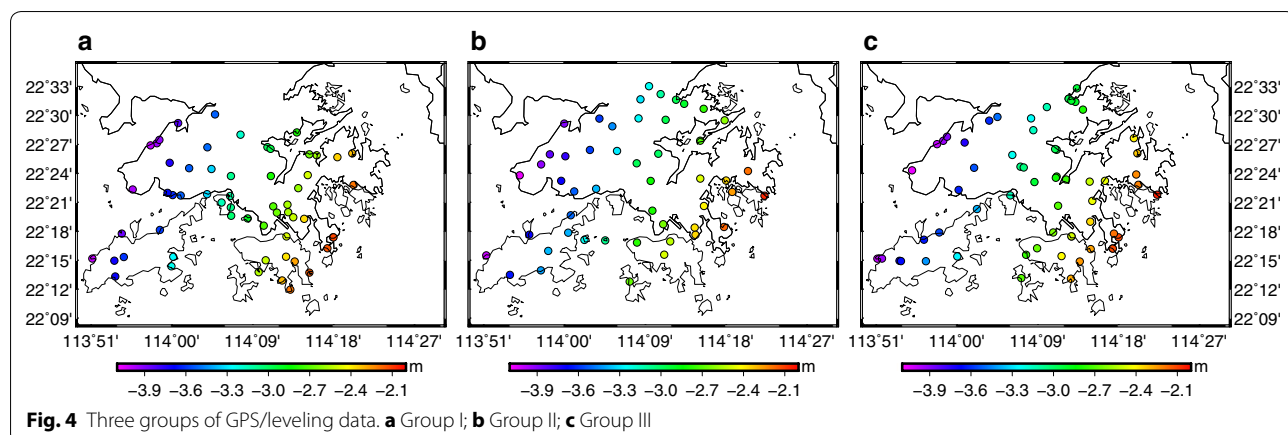


**Table 1 Statistics of the difference between altimetry and marine gravity data (Units: mGal)**

Max	Min	Mean	SD
12.6	-30.0	-4.8	4.3

The bias of the DTU13 model versus marine gravity data is at the level of 4.8 mGal, which needs to be estimated as unknown bias parameters in the functional model, as shown in Eq. (8). The imperfection in height transforming parameters and uncorrected systematic errors in the data may result in unreduced biases in the data after height unification. Thus, except for the terrestrial gravity data over Hong Kong, terrestrial data in Shenzhen and all shipborne and altimetry data are supposed to have biases. For data derived from specific source, we assume a constant bias parameter in the functional model, and

three bias parameters in total are estimated using the least square adjustment.

Based on RCR methodology, residual gravity data are computed by subtracting the long- and short-wavelength parts from the original observations. Figure 6 shows the residual gravity data, where (a) and (d) represent the residual terrestrial data, (b) and (e) display the residual marine data, and (c) and (f) show the residual altimetry data. The top panels, (a), (b) and (c), show the residual observations obtained by only subtracting EGM2008-derived quantities from the original data. The bottom panels, (d), (e) and (f), demonstrate the residual data derived by subtracting EGM2008-derived quantities and RTM corrections. After incorporating RTM corrections, the residual gravity field is much smoother, and the most significant improvements are found south-east of Shenzhen, in New Territory, Lan Tau and Hong Kong land, regions with a tendency toward topographical variation (Fig. 3). As shown in Table 2, the standard deviation (SD) of the residual terrestrial data is reduced from 11.9 to 4.4 mGal, with approximately 63% improvement after incorporating the RTM reductions. For marine data, the improvement is not as much as the terrestrial data, the SD of shipborne data is only reduced from 7.2 to 6.0 mGal, mainly due to the low resolution of the bathymetry model, the GECBO model has a spatial resolution of  $30'' \times 30''$ , and the small variation in local bathymetry (Fig. 3). Similarly, the SD of altimetry data is only reduced from 2.3 to 1.4 mGal with RTM reductions.

## Numerical results

### Determination the regularization matrix and regularization parameter

We put the Poisson wavelets on a Fibonacci grid beneath the topography, keeping it parallel with the topography (Tenzer et al. 2012). However, as mentioned above, data gaps in the observations usually lead to an ill-conditioned

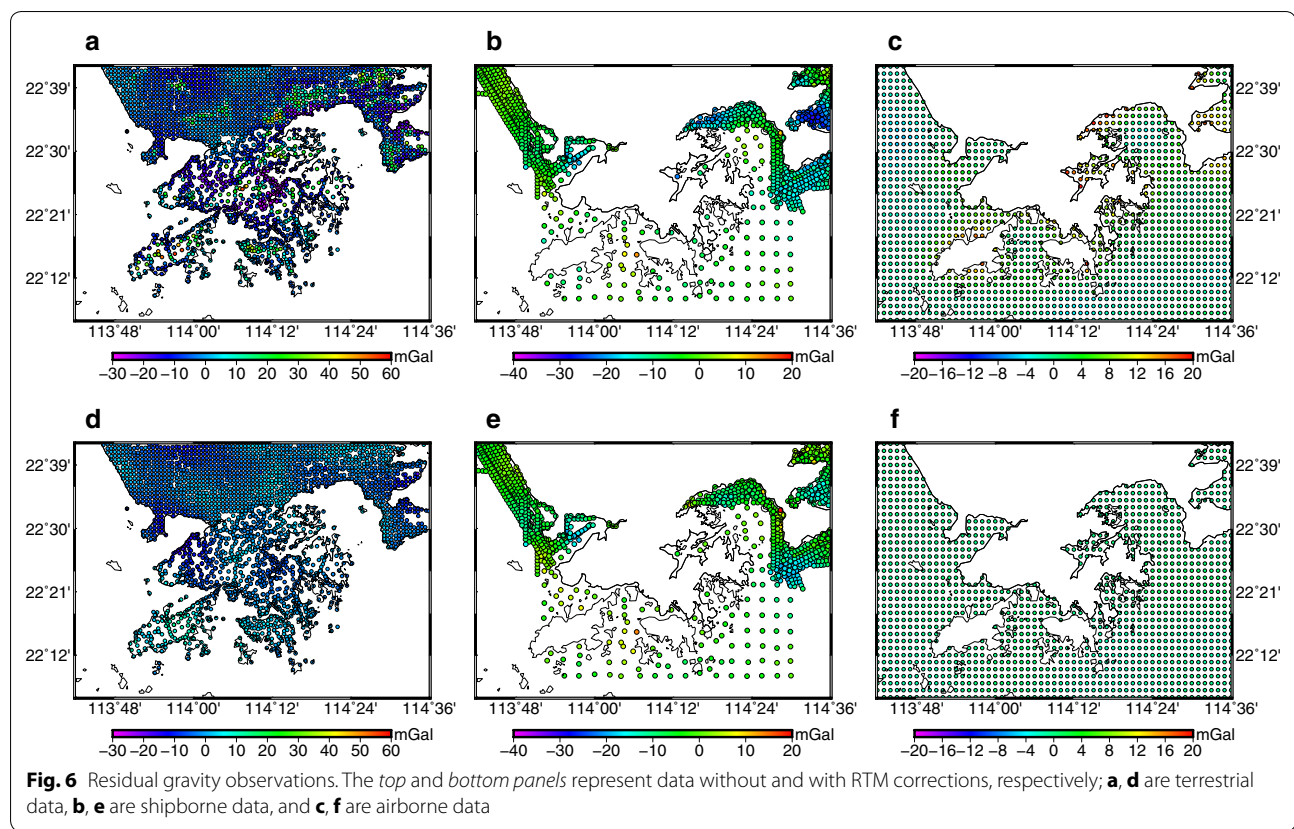


**Table 2 Statistics of the residual gravity observations (Units: mGal)**

	Max	Min	Mean	SD
Terrestrial $\Delta g - \Delta g_{\text{EGM2008}}$	57.2	-29.5	-3.0	11.9
Terrestrial $\Delta g - \Delta g_{\text{EGM2008}} - \Delta g_{\text{RTM}}$	13.7	-18.6	-1.1	4.4
Shipborne $\Delta g - \Delta g_{\text{EGM2008}}$	13.0	-30.4	-8.6	7.2
Shipborne $\Delta g - \Delta g_{\text{EGM2008}} - \Delta g_{\text{RTM}}$	12.9	-20.6	-5.7	6.0
Satellite altimetry $\Delta g - \Delta g_{\text{EGM2008}}$	18.9	-10.9	-0.8	2.3
Satellite altimetry $\Delta g - \Delta g_{\text{EGM2008}} - \Delta g_{\text{RTM}}$	9.8	-8.8	-0.1	1.4

least squares system. Thus, before computing a high-quality model, the reliability of the L-curve approach and performances of various regularization matrices need to be evaluated. The numerical experiment is designed as follows, the grid depth is selected as 40 km, and the number of Poisson wavelets is approximately chosen as 1600. Terrestrial, shipboard and altimetry gravity data, as well as the two groups of GPS/leveling data (i.e., group I and II), are combined for modeling. The normal matrix with this parameterization is highly ill-conditioned, which is the proper case study for investigating the performances of the Tikhonov regularization technique. Figure 7 shows L-curve plots for various regularization matrices, where

the optimal regularization parameter is between  $10^{-11}$  and  $10^{-10}$  when zero-order regularization is applied. For the first-order regularization, both for the radial and horizontal constrained matrices, the optimal parameter is situated between  $10^{-12}$  and  $10^{-11}$ . To further demonstrate the L-curve corner, the regularization parameters are densified around the intervals where optimal parameters are located (red circles in Fig. 7); the corresponding information can be found in Tables 3 and 4. The estimated optimal regularization parameters for zero- and first-order regularization matrices are  $\alpha = 10^{-10.6}$  and  $\alpha = 10^{-11.3}$ , respectively. However, the L-curve method may lead to obtain an over-smoothed solution (Xu 1998). Therefore, we also provide the quality of various solutions using an external validation from the GPS/leveling data from group III, (Tables 3, 4). These results indicate that the optimal parameters estimated from the L-curve method are consistent with the direct evaluation results, suggesting the L-curve method in this study is reliable. In addition, there are no differences in the performances of different first-order regularization matrices, i.e., the radial and horizontal constrained matrices, and thus we do not distinguish these matrices in the following discussion. However, when comparing the quality of solutions derived from zero- and first-order regularization, we

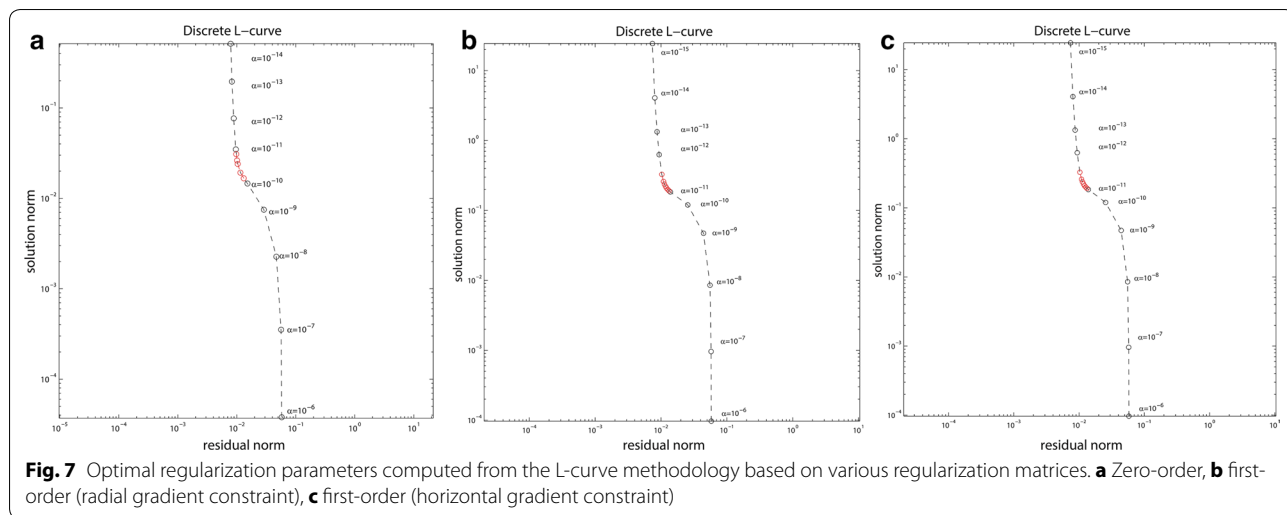


**Table 3 Evaluation of different geoids with various regularization parameters when zero-order regularization is used (Units: cm)**

Regularization parameters	$10^{-14}$	$10^{-13}$	$10^{-12}$	$10^{-11}$	$10^{-10.8}$	$10^{-10.7}$	$10^{-10.6}$	$10^{-10.4}$	$10^{-10.2}$	$10^{-10}$	$10^{-9}$	$10^{-8}$	$10^{-7}$
	2.8	2.5	2.3	2.1	2.0	1.9	1.8	1.9	2.0	2.2	2.4	2.6	3.0

**Table 4 Evaluation of different geoids with various regularization parameters when first-order regularization is used (Units: cm)**

Regularization parameters	$10^{-14}$	$10^{-13}$	$10^{-12}$	$10^{-11.8}$	$10^{-11.6}$	$10^{-11.4}$	$10^{-11.3}$	$10^{-11.2}$	$10^{-11}$	$10^{-10}$	$10^{-9}$	$10^{-8}$	$10^{-7}$
Radial constraint	2.4	2.2	2.1	1.9	1.8	1.7	1.6	1.7	1.7	1.8	1.9	2.1	2.3
Horizontal constraint	2.4	2.2	2.1	1.9	1.8	1.7	1.6	1.7	1.7	1.8	1.9	2.1	2.3

conclude the application of first-order regularization produces better results, and the accuracy of the corresponding model reaches 1.6 cm. In comparison, for solutions computed from zero-order regularization, the accuracy decreases to 1.8 cm. These results show the choice of regularization matrices has a non-negligible effect on the solutions, and the first-order regularization may be more preferable for local gravity field modeling.

#### Optimal network design for Poisson wavelets

Another key point affecting the final solution quality is the network design of the Poisson wavelets, where the optimal depth and number of Poisson wavelets need to be carefully estimated (Wu et al. 2016). The depth should not be chosen too shallow, which may lead to overfitting problem. However, too deep Poisson wavelets may cause a heavily ill-conditioned normal matrix, where strong regularization is needed, and the associated regularization errors may corrupt the solution. A good depth choice should be a trade-off between data fit and smoothness

of the solution (Slobbe 2013). In addition to depth, the number of Poisson wavelets also affects the stability and the quality of the solution. To obtain the optimal network design, we use a trial-and-error approach, i.e., preselected depths and number of Poisson wavelets are combined to form various networks; based on these networks, different solutions are computed. For selecting the best solution, GPS/leveling points serve as evaluation data, where the combination of the depth and number that obtains the best fit to the evaluation data is the optimal parameterization. Through trial and error, the depth of the grid was found to increase from 10 to 40 km with an interval of 5 km, and the number of Poisson wavelets in the computational domain changed from 400 to 2000 with an increment of 400. Similar to the case study designed in the previous section, the first two GPS/leveling groups, together with the heterogeneous gravity data, are incorporated for gravity field modeling. The third group of GPS/leveling serves as evaluation data for validating the different solutions. Finally, the L-curve approach with

first-order Tikhonov regularization is applied for managing the ill-conditioned system. Figure 8 shows the quality of the different models parameterized using various networks, where a minimum SD of 1.1 cm is obtained when the depth is 10 km and the number is 1600. Adding more Poisson wavelets only increases the computational load, without gaining improvement, e.g., the accuracy of the geoid decreases to 1.2 cm when the depth is unchanged, but the number increases to 2000. We also note that there are other choices that provide slightly worse solutions with a SD value a few millimeters larger than 1.1 cm, which indicates the solution is quite robust with respect to minor changes in network parameterization.

#### A new height reference surface over Hong Kong

Based on the optimal network designed above, a new height reference surface, HKGEOID-2016, over Hong Kong is estimated. Figure 9 provides the estimated biases for the gravity data, with magnitudes of  $-0.6$ ,  $-0.7$  and  $-4.5$  mGal for terrestrial, shipborne and altimetry data, respectively. However, the estimated bias in the altimetry data is not exactly consistent with the results shown in Table 1, where the bias between shipborne measurements and altimetry data is roughly  $-4.8$  mGal. This also indicates the biases estimated from the functional model parameterized in this study may deviate from the true value, and additional efforts are needed for further improvements in the near future. Figure 10 displays the residuals of the gravity observations after the least squares adjustment. As shown in Table 5, the functional model fits the terrestrial and marine data much better than the altimetry data, and the SD of the residuals for terrestrial and marine data is approximately 1.2 and

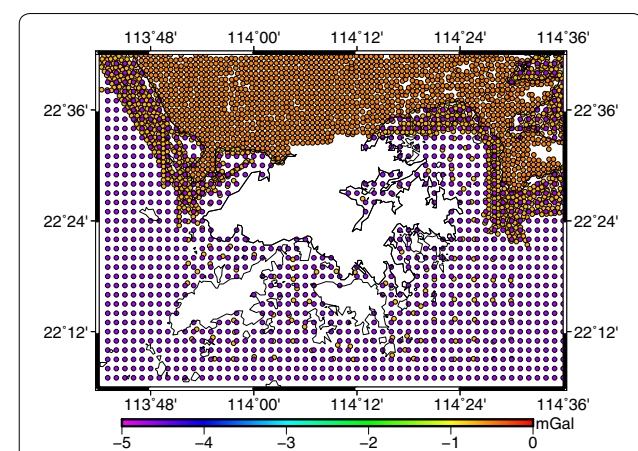


**Fig. 9** Estimated biases for heterogeneous gravity data

1.1 mGal, respectively, while for altimetry data this value significantly increases to 4.8 mGal. In addition, the most prominent residuals in the altimetry data are located at coastal areas, which further demonstrates the poor DTU13 quality over these regions. Moreover, we conclude that the parameterization of the functional model with constant unknown bias parameters does not thoroughly remove systematic errors in the data. Future work should also incorporate densification of shipborne gravity measurements, which may further improve the solution quality over marine areas. Further, for the two groups of GPS/leveling data used to combine the gravimetric solution and GPS/leveling data, i.e., groups I and II, the residuals are displayed in Fig. 11, and the corresponding statistics are provided in Table 6. These results show the internal agreement between the model and GPS/leveling data. For comparison, we also provide results derived from the purely gravimetric geoid, i.e., the solution modeled only from gravity data using Poisson wavelets. The corresponding results display differences between the purely gravimetric solution and GPS/leveling data at the decimeter level, ranging from 6.7 to 22.3 cm. SD values are 4.1 and 3.6 cm, and mean values are 15.1 and 15.4 cm for groups I and II, respectively. These statistics indicate systematic errors exist between these two data sets. Because the GPS/leveling data are acquired using high-quality GPS measurements and spirit leveling observations, it is usually hypothesized that errors in the computed gravimetric model primarily account for the observed systematic errors; these are usually due to commission errors in the GGM, as well as uncorrected systematic errors in the data. However, as shown in Table 6, the incorporation of two groups of GPS/leveling data leads to a significant reduction in SD values for differences between the modeled geoid heights and observed

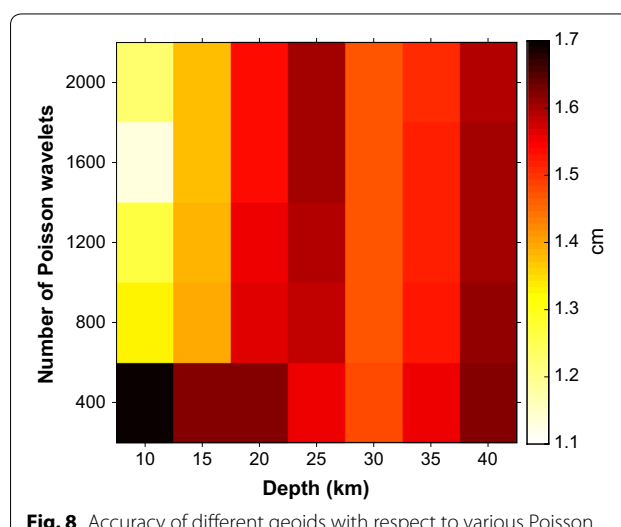


**Fig. 8** Accuracy of different geoids with respect to various Poisson wavelet networks

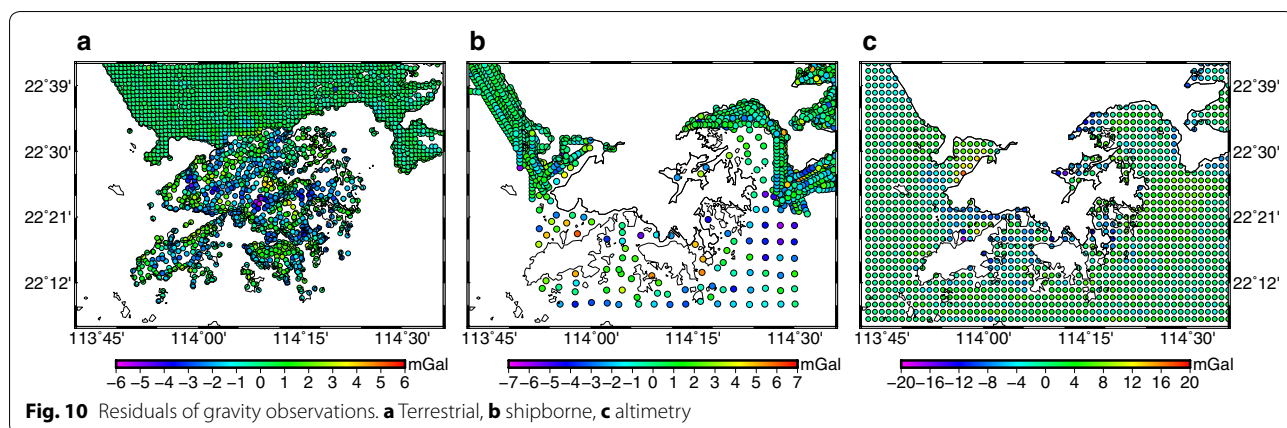


**Table 5 Statistics of the residuals of gravity data (Units: mGal)**

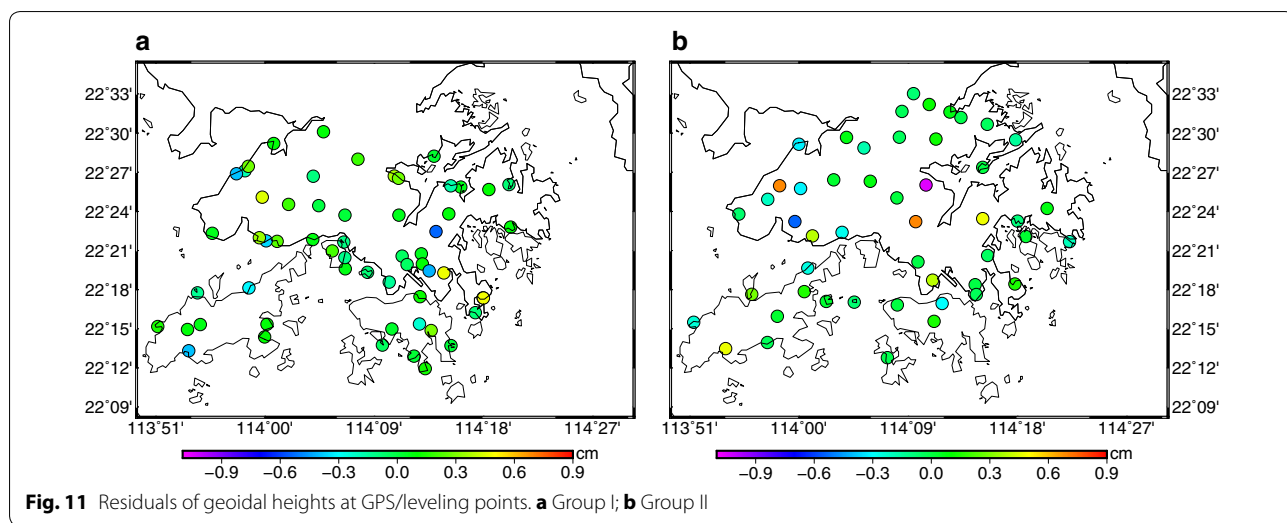
	Max	Min	Mean	SD
Terrestrial	5.0	-5.7	0.0	1.2
Marine	5.6	-6.3	0.0	1.1
Satellite altimetry	15.4	-18.4	0.0	4.8

**Table 6 Statistics of the residuals of geoidal heights at GPS/leveling points (Units: cm)**

	Max	Min	Mean	SD
Group I	0.5	-0.6	0.0	0.2
Group II	0.8	-1.1	0.0	0.3

ones, to 0.2 and 0.3 cm for groups I and II, respectively. More important, introducing these GPS/leveling data substantially reduces the mean difference between the model and GPS/leveling data. The zero mean values for both groups of data also indicate that the gravimetric model and GPS/leveling data can be properly combined through the direct approach we proposed. Furthermore, systematic errors, especially in the computed model, have been significantly reduced when compared to the case derived from a purely gravimetric solution.

Results from the GPS/leveling data for groups I and II only provide the internal agreement between the modeled geoid and GPS/leveling data, and cannot be used for assessing the solution quality because they are used as observations for modeling. Thus, the third group of GPS/leveling data, with independent 61 point-wise measurements, is used for external validation and the result is displayed in Fig. 12. All residuals are within 2.0 cm (Table 7), the SD of the differences between the HKGEOD-2016 and GPS/leveling points is approximately 1.1 cm, and the zero mean value also confirms the geoid model and



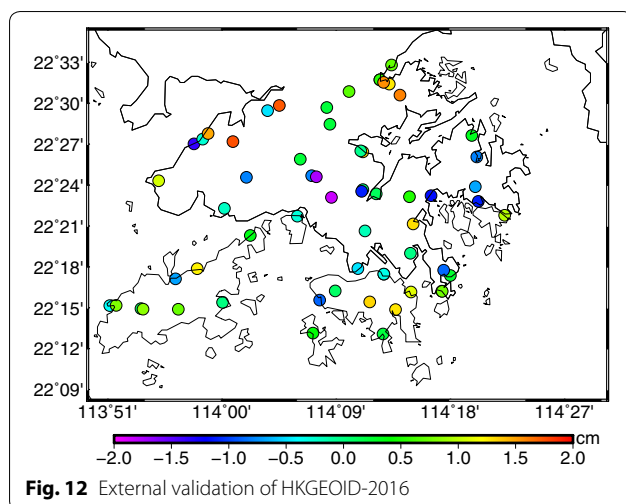


**Table 7** External accuracy of HKGEOID-2016 (Units: cm)

Max	Min	Mean	SD
1.8	-1.9	0.0	1.1

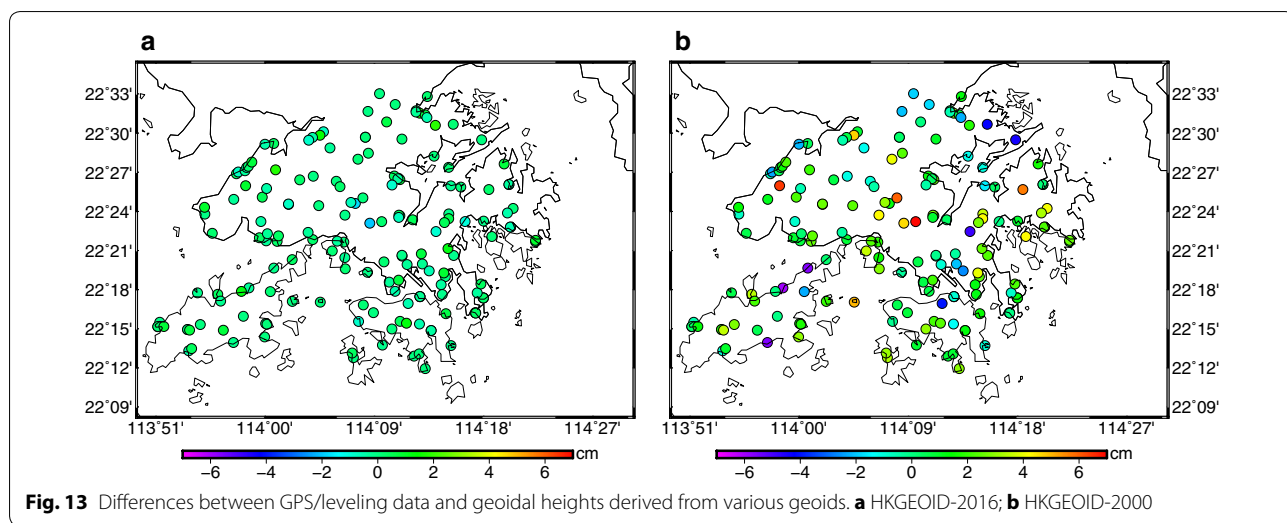
GPS/leveling data have been combined properly. For further evaluation, we also compare HKGEOID-2016 with the existing model, HKGEOID-2000 (Luo et al. 2005). Figure 13 shows the differences between the observed and computed geoidal heights at all GPS/leveling points based on the various geoids. Compared to the solution derived from HKGEOID-2000, as shown in the Table 8, the SD of these differences is reduced from 2.4 to 0.6 cm when HKGEOID-2016 is incorporated. We mainly attribute these improvements to the incorporation of

**Table 8** Statistical differences between GPS/leveling data and geoidal heights based on various geoids (Units: cm)

	Max	Min	Mean	SD
HKGEOID-2016	1.8	-1.9	0.0	0.6
HKGEOID-2000	6.9	-6.0	0.8	2.4

more gravity-related observations, as well as recent leveling network adjustments to reduce the systematic errors in the leveling system over Hong Kong. We also note that the mean value of the residuals is 0.8 cm when HKGEOID-2000 is used, which indicates systematic errors may exist in the original GPS/leveling data used by Luo et al. (2005).

The performances of the recently published GGMs are also investigated in Hong Kong, i.e., EGM2008 with d/o 2190 (Pavlis et al. 2012), EIGEN-6C3STAT (d/o 1949) and EIGEN-6C4 (d/o 2190) (Förste et al. 2012, 2014) (Fig. 14). The statistics in Table 9 show the accuracy of these GGMs is not better than 4 cm, and the mean deviation between GGM and local geoid is larger than 17 cm, which is undesirable for engineering purposes or geo-physical investigation. The main reason for the poor performances of these GGMs is their development was implemented without confidential gravity data from China, and the quality of these models in regions such as China is suspect, and local refinements are necessary. Moreover, differences between the HKGEOID-2016 and GGM-derived geoids are shown in Fig. 15, these differences are at the decimeter level, and the incorporation of locally distributed data primarily contributes to improving the fine structures of the regional gravity field at short scales.



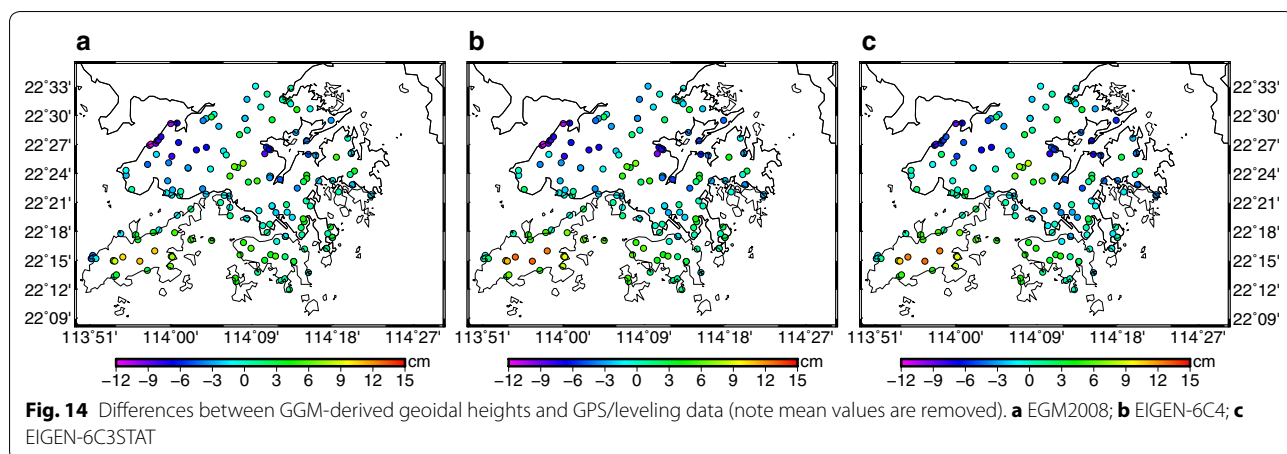


**Table 9 Statistical differences between GPS/leveling data and GGM-derived geoidal heights (Units: cm)**

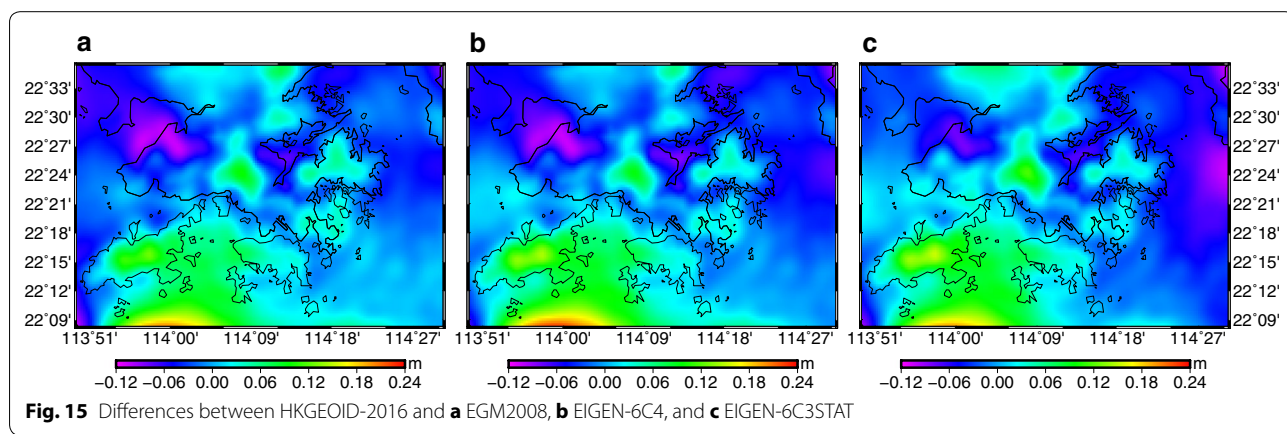
	Mean	SD
EGM2008	17.8	4.2
EIGEN-6C4	20.4	4.5
EIGEN-6C3STAT	23.3	4.2

## Conclusions

Poisson wavelets are used for modeling the regional gravity field using data from various observational techniques. The method combines data with different spatial coverage, various noise levels, and spectral contents. As a case study, terrestrial, shipborne, and satellite altimetry gravity data, as well as GPS/leveling measurements, are incorporated in the Poisson wavelet model for regional gravity field recovery over Hong Kong.

The Tikhonov regularization is introduced to manage the ill-conditioned least squares system; in particular, the performances of various regularization matrices

are investigated. The numerical results show solutions with first-order regularization provide better results, where the accuracy of the local solution increases by 0.2 cm compared to that obtained from zero-order regularization. These results also indicate that first-order regularization may be more preferable in regional gravity field recovery using Poisson wavelets. Moreover, a direct approach is proposed to properly combine the gravimetric quasi-geoid/geoid and GPS/leveling data; a subset of the GPS/leveling data is treated as an independent observation group to formulate the new functional model, and the quasi-geoid/geoid that fits the local leveling system can be modeled in a single step. The results show the SD is approximately 0.3 cm for the residuals on the first two GPS/leveling groups, regarded as observations. The zero mean value indicates the gravimetric model and GPS/leveling data can be properly combined through this direct approach. In addition, an external validation with 61 independent GPS/leveling points shows that the accuracy of the new geoid, HKGEOD-2016, is approximately 1.1 cm. Compared with the original



solution, HKGEOID-2000, the SD of the differences between observed and computed geoidal heights at all GPS/leveling points is reduced from 2.4 to 0.6 cm when HKGEOID-2016 is incorporated. This is a significant improvement. In addition, the performances of three recently published GGMs, EGM2008, EIGEN-6C3STAT and EIGEN-6C4, are investigated in Hong Kong. The corresponding results show the accuracies of these GGMs are all below 4 cm. The deviation from the local geoid at the decimeter level also indicates the GGM alone cannot recover a high-quality gravity field in this region, and local refinement is necessary.

Several issues should be carefully considered to make further improvements to the local geoid. Usually, the geoid is poorly modeled in the coastal areas due to unfavorable data coverage (Hipkin et al. 2004; Filmer and Featherstone 2012). In the study region, the distribution of shipborne data is quite sparse, and the quality of the altimetry data degrades in the vicinity of coastal areas. Therefore, the densification of shipborne data would further improve the local geoid in future work. In addition, the developments of appropriate altimeter waveform retracking approaches may also contribute to improving the geoid over coastal areas (Hwang et al. 2006; Andersen and Knudsen 2009). Errors in the GGM inevitably propagate into regional solutions because we usually consider the GGM as error-free data implemented in the remove-restore framework. The magnitude of these commission errors in the GGMs reaches the centimeter scale or larger (Pavlis et al. 2012), which should be carefully considered when computing the quasi-geoid/geoid at centimeter accuracy. These commission errors are actually calibrated with GPS/leveling data using the direct approach proposed in this study. However, the errors in the GGM could also be quantified if the full error variance–covariance matrix of the spherical coefficients is known, and a more realistic error variance–covariance matrix of the data could be estimated through error propagation. In this manner, the weights of different observation groups may be more properly determined, and the accuracy of the quasi-geoid/geoid, especially for the purely gravimetric one, may be further improved.

## Abbreviations

GPS: Global Positioning System; GGM: global geopotential model; GRACE: Gravity Field and Climate Experiment; GOCE: Gravity Field and Steady-State Ocean Circulation Explorer; LSC: least squares collocation; VCE: variance component estimation; EIGEN: European Improved Gravity Model of the Earth by New Techniques; RCR: remove-compute-restore; RTM: residual terrain model; 3-D: three dimensional; DTU: Technical University of Denmark; d/o: degree and order; DTM: digital terrain model; SRTM: Shuttle Radar Topography Mission; GEBCO: General Bathymetric Chart of the Oceans; MES: mean elevation surface.

## Authors' contributions

YW and ZL initiated the study, designed the numerical experiments, and wrote the manuscript. WC and YC provided the data and supplied beneficial suggestions. YW finalized the manuscript. All authors read and approved the final manuscript.

## Author details

<sup>1</sup> MOE Key Laboratory of Fundamental Physical Quantities Measurement, School of Physics, Huazhong University of Science and Technology, Wuhan 430079, China. <sup>2</sup> Collaborative Innovation Center for Geospatial Technology, Wuhan University, Wuhan 430079, Hubei, China. <sup>3</sup> Department of Land Surveying and Geo-Informatics, Hong Kong Polytechnic University, Hung Hom 999077, Hong Kong, China.

## Acknowledgements

The authors would like to give our sincerest thanks to the two anonymous reviewers for their beneficial suggestions and comments, which helped us improve the manuscript. We would also like to thank the anonymous editor and the editorial office for their work on language editing. We acknowledge the assistance of Prof. Roland Klees and Dr. Cornelis Slobbe from Delft University of Technology for kindly providing the original software. This research was primarily supported by the National Natural Science Foundation of China (41374023), China Postdoctoral Science Foundation (No. 2016M602301), Key Laboratory of Geospace Environment and Geodesy, Ministry of Education, Wuhan University (15-02-08), the State Scholarship Fund from Chinese Scholarship Council (201306270014) and project K-ZS0J, 'Development of a Hong Kong Positioning Infrastructure based on GPS, Beidou, and Ground based Augmentation System.' Generic Mapping Tools (GMT) was used to generate the figures.

## Competing interests

The authors declare that they have no competing interests.

Received: 8 November 2016 Accepted: 13 February 2017

Published online: 24 February 2017

## References

- Andersen OB, Knudsen P (2009) The DNSC08 mean sea surface and mean dynamic topography. *J Geophys Res* 114(C11):327–343. doi:[10.1029/2008JC005179](https://doi.org/10.1029/2008JC005179)
- Andersen OB, Knudsen P, Stenseng L (2013) The DTU13 global mean sea surface from 20 years of satellite altimetry. In: OSTST Meeting, Boulder, Colo
- Bentel K, Schmidt M, Gerlach C (2013) Different radial basis functions and their applicability for regional gravity field representation on the sphere. *Int J Geomath* 4(1):67–96. doi:[10.1007/s13137-012-0046-1](https://doi.org/10.1007/s13137-012-0046-1)
- Chambodut A, Panet I, Mandea M, Diament M, Holschneider M, Jamet O (2005) Wavelet frames: an alternative to spherical harmonic representation of potential fields. *Geophys J Int* 163(3):875–899. doi:[10.1111/j.1365-246X.2005.02754.x](https://doi.org/10.1111/j.1365-246X.2005.02754.x)
- Chen Y, Luo Z (2004) A hybrid method to determine a local geoid model—Case study. *Earth Planets Space* 56(4):419–427. doi:[10.1186/BF03352495](https://doi.org/10.1186/BF03352495)
- Eshagh M, Zoghi S (2016) Local error calibration of EGM08 geoid using GNSS/levelling data. *J Appl Geophys* 130(5):209–217. doi:[10.1016/j.jappgeo.2016.05.002](https://doi.org/10.1016/j.jappgeo.2016.05.002)
- Evans RB (1990) Hong Kong gravity observations in July 1990 with BGS Lacoste and Romberg meter No. 97 and international connections to IGSN 71. Report, British and Geology Survey, Hong Kong, China
- Featherstone WE (2000) Refinement of a gravimetric geoid using GNSS and levelling data. *J Surv Eng* 126(2):27–56. doi:[10.1061/\(ASCE\)0733-9453\(2000\)126:2\(27\)](https://doi.org/10.1061/(ASCE)0733-9453(2000)126:2(27))
- Filmer MS, Featherstone WE (2012) A re-evaluation of the offset in the Australian Height Datum between mainland Australia and Tasmania. *Mar Geod* 35(1):107–119. doi:[10.1080/01490419.2011.634961](https://doi.org/10.1080/01490419.2011.634961)
- Forsberg R (1984) A study of terrain reductions, density anomalies and geophysical inversion methods in gravity field modeling. Report No. 355,

- Department of Geodetic Science and Surveying, The Ohio State University, Columbus, Ohio, USA
- Forsberg R, Tscherning CC (1981) The use of height data in gravity field approximation by collocation. *J Geophys Res* 86(B9):7843–7854
- Förste C, Bruinsma SL, Flechtner F, Marty JC, Lemoine JM, Dahle C, Abrikosov O, Neumayer KH, Biancale R, Barthelmes F, Balmino G (2012) A preliminary update of the Direct approach GOCE Processing and a new release of EIGEN-6C. AGU General Assembly, San Francisco
- Förste C, Bruinsma SL, Abrikosov O, Lemoine JM, Schaller T, Götze HJ, Ebbing J, Marty JC, Flechtner F, Balmino G, Biancale R (2014) EIGEN-6C4 The latest combined global gravity field model including GOCE data up to degree and order 2190 of GFZ Potsdam and GRGS Toulouse. The 5th GOCE User Workshop, Paris, France
- Fotopoulos G (2005) Calibration of geoid error models via a combined adjustment of ellipsoidal, orthometric and gravimetric geoid height data. *J Geod* 79(1):111–123. doi:[10.1007/s00190-005-0449-y](https://doi.org/10.1007/s00190-005-0449-y)
- Hansen PC, Jensen TK, Rodriguez G (2007) An adaptive pruning algorithm for the discrete L-curve criterion. *J Comput Appl Math* 198(2):483–492. doi:[10.1016/j.cam.2005.09.026](https://doi.org/10.1016/j.cam.2005.09.026)
- Hayn M, Panet I, Diamant M, Holschneider M, Mandea M, Davaille A (2012) Wavelet-based directional analysis of the gravity field: evidence for large-scale undulations. *Geophys J Int* 189(3):1430–1456. doi:[10.1111/j.1365-246X.2012.05455.x](https://doi.org/10.1111/j.1365-246X.2012.05455.x)
- Heck B, Seitz K (2007) A comparison of the tesseroid, prism and point-mass approaches for mass reductions in gravity field modelling. *J Geod* 81(2):121–136. doi:[10.1007/s00190-006-0094-0](https://doi.org/10.1007/s00190-006-0094-0)
- Heiskanen WA, Moritz H (1967) Physical geodesy. WH Freeman and Co, San Francisco
- Hipkin RG, Haines K, Beggan C, Bingley R, Hernandez F, Holt J, Baker T (2004) The geoid EDIN2000 and mean sea surface topography around the British Isles. *Geophys J Int* 157(2):565–577. doi:[10.1111/j.1365-246X.2004.01989.x](https://doi.org/10.1111/j.1365-246X.2004.01989.x)
- Holschneider M, Iglesias-Nowak I (2004) Poisson wavelets on the sphere. *J Fourier Anal Appl* 13(4):405–419. doi:[10.1007/s00041-006-6909-9](https://doi.org/10.1007/s00041-006-6909-9)
- Hwang C, Guo J, Deng X, Hsu H, Liu Y (2006) Coastal gravity anomalies from retracked geosat/GM altimetry: improvement, limitation and the role of airborne gravity data. *J Geod* 80(4):204–216. doi:[10.1007/s00190-006-0052-x](https://doi.org/10.1007/s00190-006-0052-x)
- Jiang T, Wang YM (2016) On the spectral combination of satellite gravity model, terrestrial and airborne gravity data for local gravimetric geoid computation. *J Geod*. doi:[10.1007/s00190-016-0932-7](https://doi.org/10.1007/s00190-016-0932-7)
- Klees R, Prutkin I (2008) The combination of GNSS-levelling data and gravimetric (quasi-) geoid heights in the presence of noise. *J Geod* 84(12):731–749. doi:[10.1007/s00190-010-0406-2](https://doi.org/10.1007/s00190-010-0406-2)
- Klees R, Tenzer R, Prutkin I, Wittwer T (2008) A data-driven approach to local gravity field modelling using spherical radial basis functions. *J Geod* 82(8):457–471. doi:[10.1007/s00190-007-0196-3](https://doi.org/10.1007/s00190-007-0196-3)
- Koch KR, Kusche J (2002) Regularization of geopotential determination from satellite data by variance components. *J Geod* 76(5):259–268. doi:[10.1007/s00190-002-0245-x](https://doi.org/10.1007/s00190-002-0245-x)
- Kuroishi Y (2009) Improved geoid model determination for Japan from GRACE and a regional gravity field model. *Earth Planets Space* 61(7):807–813. doi:[10.1186/BF03353191](https://doi.org/10.1186/BF03353191)
- Kusche J (2003) A Monte-Carlo technique for weight estimation in satellite geodesy. *J Geod* 76(11):641–652. doi:[10.1007/s00190-002-0302-5](https://doi.org/10.1007/s00190-002-0302-5)
- Kusche J, Klees R (2002) Regularization of gravity field estimation from satellite gravity gradients. *J Geod* 76(6):359–368. doi:[10.1007/s00190-002-0257-6](https://doi.org/10.1007/s00190-002-0257-6)
- Lieb V, Schmidt M, Dettmering D, Börger K (2016) Combination of various observation techniques for regional modeling of the gravity field. *J Geophys Res Solid Earth* 121(5):3825–3845. doi:[10.1002/2015JB012586](https://doi.org/10.1002/2015JB012586)
- Luo Z, Ning J, Chen Y, Yang Z (2005) High precision geoid models HKGEOD-2000 for Hong Kong and SZGEOID-2000 for Shenzhen, China. *Mar Geod* 28(2):191–200. doi:[10.1080/01490410590953758](https://doi.org/10.1080/01490410590953758)
- Nahavandchi N, Soltanpour A (2006) Improved determination of heights using a conversion surface by combining gravimetric quasi-geoid/geoid and GNSS-levelling height differences. *Stud Geophys Geod* 50(2):165–180. doi:[10.1007/s11200-006-0010-3](https://doi.org/10.1007/s11200-006-0010-3)
- Odera PA, Fukuda Y (2014) Improvement of the geoid model over Japan using integral formulae and combination of GGMs. *Earth Planets Space* 66(1):1–7. doi:[10.1186/1880-5981-66-22](https://doi.org/10.1186/1880-5981-66-22)
- Omang OCD, Forsberg R (2000) How to handle topography in practical geoid determination: three examples. *J Geod* 74(6):458–466. doi:[10.1007/s001900000107](https://doi.org/10.1007/s001900000107)
- Panet I, Kuroishi Y, Holschneider M (2011) Wavelet modelling of the gravity field by domain decomposition methods: an example over Japan. *Geophys J Int* 184(1):203–219. doi:[10.1111/j.1365-246X.2010.04840.x](https://doi.org/10.1111/j.1365-246X.2010.04840.x)
- Pavlis NK, Factor JK, Holmes SA (2007) Terrain-related gravimetric quantities computed for the next EGM. Proceedings of the 1st international symposium of the international gravity field service, Istanbul, pp. 318–323
- Pavlis NK, Holmes SA, Kenyon SC, Factor JF (2008) An Earth gravitational model to degree 2,160: EGM2008. Presented at the 2008 General Assembly of the European Geosciences Union, Vienna, April 13–18
- Pavlis NK, Holmes SA, Kenyon SC, Factor JF (2012) The development and evaluation of Earth Gravitational Model (EGM2008). *J Geophys Res* 117:B04406. doi:[10.1029/2011JB008916](https://doi.org/10.1029/2011JB008916)
- Prutkin I, Klees R (2008) On the non-uniqueness of local quasi-geoids computed from terrestrial gravity anomalies. *J Geod* 82(3):147–156. doi:[10.1007/s00190-007-0161-1](https://doi.org/10.1007/s00190-007-0161-1)
- Rummel R, Balmino G, Johannessen J, Visser P, Woodworth P (2002) Dedicated gravity field missions—Principle and aims. *J Geodyn* 33(1):3–20. doi:[10.1016/S0264-3707\(01\)00050-3](https://doi.org/10.1016/S0264-3707(01)00050-3)
- Shih HC, Hwang C, Barriot JP, Mouyen M, Corréa P, Lequeux D, Sichou L (2015) High-resolution gravity and geoid models in Tahiti obtained from new airborne and land gravity observations: data fusion by spectral combination. *Earth Planets Space* 67(1):1–16. doi:[10.1186/s40623-015-0297-9](https://doi.org/10.1186/s40623-015-0297-9)
- Slobbe DC (2013) Roadmap to a mutually consistent set of offshore vertical reference frames. Dissertation, Delft University of Technology, Delft
- Tapley BD, Bettadpur S, Watkins M, Reigber C (2004) The gravity recovery and climate experiment: mission overview and early results. *Geophys Res Lett* 31:L09607. doi:[10.1029/2004GL019920](https://doi.org/10.1029/2004GL019920)
- Tenzer R, Klees R (2008) The choice of the spherical radial basis functions in local gravity field modeling. *Stud Geophys Geod* 52(3):287–304. doi:[10.1007/s11200-008-0022-2](https://doi.org/10.1007/s11200-008-0022-2)
- Tenzer R, Klees R, Wittwer T (2012) Local gravity field modelling in rugged terrain using spherical radial basis functions: case study for the Canadian rocky mountains. In: Kenyon S (eds) *Geodesy for Planet Earth*, International Association of Geodesy Symposia 136, Springer, Berlin, pp 401–409
- Tscherning CC (1978) Introduction to functional analysis with a view to its application in approximation theory. In: Moritz H, Sünkel H (eds) Approximation methods in geodesy. Karlsruhe, Germany
- Wang Y, Saleh J, Li X, Roman DR (2012) The US Gravitational Geoid of 2009 (USGG2009): model development and evaluation. *J Geod* 86(3):165–180. doi:[10.1007/s00190-011-0506-7](https://doi.org/10.1007/s00190-011-0506-7)
- Wittwer T (2009) Regional gravity field modelling with radial basis functions, Dissertation, Delft University of Technology, Delft
- Wu Y, Luo Z (2016) The approach of regional geoid refinement based on combining multi-satellite altimetry observations and heterogeneous gravity data sets. *Chin J Geophys (in Chinese)* 59(5):1596–1607. doi:[10.6038/cjg20160505](https://doi.org/10.6038/cjg20160505)
- Wu Y, Luo Z, Zhou B (2016) Regional gravity modelling based on heterogeneous data sets by using Poisson wavelets radial basis functions. *Chin J Geophys (in Chinese)* 59(3):852–864. doi:[10.6038/cjg20160308](https://doi.org/10.6038/cjg20160308)
- Xu P (1992) The value of minimum norm estimation of geopotential fields. *Geophys J Int* 111(1):170–178. doi:[10.1111/j.1365-246X.1992.tb00563.x](https://doi.org/10.1111/j.1365-246X.1992.tb00563.x)
- Xu P (1998) Truncated SVD methods for discrete linear ill-posed problems. *Geophys J Int* 135(2):505–514. doi:[10.1046/j.1365-246X.1998.00652.x](https://doi.org/10.1046/j.1365-246X.1998.00652.x)